Supplemental Methods:

Choice of species:

We selected 56 species of Malawi and Tanganyika cichlids for filming and UCE sequencing. We attempted to strike a balance between availability in the aquarium trade or via cichlid hobbyists, coverage of major tribes and ecotypes in each lake, and inclusion of potential independent transitions between suction feeding and biting.

Kinematics:

For filming, we housed between three and sixteen cichlids in 106L aquaria filtered with commercial air-driven sponge filters. We recorded kinematic sequences on a Fastec HiSpec 1 system (San Diego, CA, USA) at 2000 frames per second using a 120W halogen light to illuminate the tank from the side during recording. We introduced live prey (larval mosquitoes in the genus *Culex*) singly into the tank via pipette and obtained between eight and twenty kinematic sequences per individual. After each feeding trial, we placed a ruler in the same focal plane for scale. We waited at least 24 hours before using the same individual in another feeding trial. After filming, we euthanized fish with an overdose of MS-222. We then removed fin or muscle tissue for DNA extraction, library preparation, and UCE sequencing (described below), and we stored tissues in 95% EtOH at -20 C. We used one individual per species for UCE sequencing (below).

Digitizing:

From each set of videos for a given individual, we chose one sequence in which the predator appeared to be completely lateral with respect to the camera and striking with high effort. HIgh effort strikes were identified via comparisons of mouth opening to all other kinematic sequences for that individual. We always captured images of the plateau phase (*sensu* 42) at the point immediately preceding jaw closing. From these sequences we isolated a pair of images, one at the onset of the strike before the jaws had begun to open and the other with the mouth fully opened.

We then digitized a series of four landmarks (Figure 2) on the two bones of the upper jaw, the premaxilla and maxilla, using the 'tpsDig' and 'tpsUtil' morphometrics software [46]. This set of landmarks was digitized on both the closed and the open mouth frames from each feeding sequence. We digitized the distal tip of the arm of the maxilla(landmark 1), the joint between the articular and the quadrate(landmark 2), the anterior-most tip of the premaxilla(landmark 3), and the proximal tip of the maxilla(landmark 4).

In order to capture the amount of shape change that occurred between the closed and the open mouth, we used the Procrustes distance, a common measure of shape difference. We calculated kinesis of the premaxilla, maxilla, and the lower jaw separately, using a series of three coordinates, one mobile and two fixed (landmarks 1 and 2). For our mobile landmark, we

used landmark 3 for premaxillary kinesis and landmark 4 for maxillary kinesis. We calculated the Procrustes distance from each open-closed pair of images per individual using the 'geomorph' package in R [47]. We then calculated species means by averaging the Procrustes distance of all individuals of a given species.

DNA Extraction and Library Preparation:

We extracted DNA from 56 specimen tissues stored in ethanol by cutting 10-20 mg chunks from each tissue using individually wrapped razor blades and following the Qiagen DNeasy protocol. We modified the protocol by eluting DNA from the column membrane using 65 uL of warm (50-55 °C) Buffer AE. Following elution, we quantified DNA using a Qubit fluorometer by combining 2 uL eluate with 198 uL quantification reagent and following the Qubit quantification protocol. We extracted an average of 91.2 ng DNA (95 CI: 31.8) from individual cichlid tissue samples (Table S3). Following extraction and quantification, we determined the quality of DNA extracts by visualizing 50-100 ng of each extract by electrophoresis through 1.5% (w/v) agarose gel in TBE. We then prepared 100 µL aliquots (10 ng/µL) of each sample for sonication, and we sheared each sample to 300-600 bp in length using 5-10 cycles of sonication (High; 30 s on; 90 s off) on a BioRuptor (Diagenode, Inc.).

To collect sequence data from UCEs, we followed modified versions (available from http://ultraconserved.org) of the enrichment approach initially described in [25-26] for library preparation (v1.10), target enrichment (v1.5), and post-enrichment recovery (v2.4). Briefly, we input sheared DNA to a “with-bead” library preparation process using commercial library preparation reagents (Kapa Biosystems) and a generic SPRI substitute ((Rohland & Reich 2012); hereafter SPRI). During adapter ligation, we substituted a custom-designed set of adapters that allows dual-indexing during the subsequent PCR amplification phase. Following universal adapter ligation, we amplified 50% of the library volume (~15 uL) using a reaction mix of 25 µL HiFi HotStart ReadyMix polymerase (Kapa Biosystems), 5 µL of dual-indexed primer mix (5 µM each), and 5 µL double-distilled water (ddH20) using the following thermal protocol: 98 C for 45s; 10-12 cycles of 98 C for 15s, 60 C for 30s, 72 C for 60s; and a final extension of 72 C for 5m. We purified resulting reactions using 1.8X SPRI and rehydrated libraries in 33 µL ddH2O. We quantified 2 µL of each library using a Qubit fluorometer. Following library preparation, PCR amplification, and purification, libraries contained an average of 49.7 DNA (95 CI: 1.2) in 33 µL 10 mM Tris-HCl. We selected samples for grouping based on taxonomic similarity, and we combined 62.5 ng DNA from each sample into pools of eight libraries at equimolar ratios (500 ng each pool). The final concentration of each pool was 147 ng/µL.

Library Enrichment and Sequencing:

We enriched libraries for UCE targets following the protocol described above (v1.5) with the following reagents: (1) 100 ng MYcroarray MYBaits UCE Capture Kit baits; (2) 500 ng blocking oligos designed against our custom, dual sequence indexes; (3) 500 ng of commercially available chicken Cot-1 DNA (Applied Genetics Laboratories, Inc.); and (4) 1% SDS (versus 10% SDS). Previous tests [48] have suggested the organismal source of Cot-1 DNA is not

critical to enrichment success. We ran the hybridization reaction for 24 hours at 65 C. Following hybridization we bound all pools to streptavidin-coated beads (MyOne C1, Life Technologies, Inc.) and washed bound libraries according to the protocol. Following enrichment, we removed the final aliquot of wash buffer and allowed samples to dry for five minutes while sitting in a magnet stand. We removed residual buffer, added 30 µL ddH20 to each sample, and then proceeded directly to PCR recovery while the enriched libraries were still bound to streptavidin beads. We combined 15 µL of streptavidin bead-bound, enriched library in water with 25 µL HiFi HotStart ReadyMix polymerase (Kapa Biosystems), 5 µL of Illumina TruSeq primer mix (5 µM each), and 5 µL of ddH2O. We performed PCR recovery of each library using the following thermal profile: 98 C for 45s; 16 cycles of 98 C for 15s, 60 C for 30s, 72 C for 60s; and a final extension of 72 C for 5m. We purified resulting reactions using 1.0X SPRI, and we re-hydrated enriched pools in 33 µL ddH2O. We quantified 2 µL of each enriched pool using a Qubit fluorometer, as described above. Following enrichment, PCR recovery, and purification, enriched pools contained approximately 34.0 ng DNA (95 CI: 4.6).

Prior to sequencing, we diluted PCR-recovered, enriched pools to 2.5 ng/µL, determined the fragment size distribution of each enriched pool using a Bioanalyzer (Agilent Technologies, Inc.), qPCR-quantified each pool using a commercial library quantification kit (Kapa Biosystems), and adjusted estimated library concentrations based on our qPCR results and the mean fragment size of each pool. We created an equimolar sample of all pools at 10 nM concentration for sequencing, and we sequenced the 10 nM sample of pooled libraries using approximately ⅓ of an Illumina NextSeq PE150 run (Georgia Genomics Facility). We filled the remainder of the NextSeq run with samples having sequence tags at both 5' and 3' ends of the library construct that were completely different from any tags we applied to our cichlid samples.

Analysis of UCE data:

We converted BCL data to FASTQ data using bcl2fastq2 (v02.14.01.07, Illumina Inc.), and we merged read data for each sample from the four NextSeq lanes into two FASTQ files representing Read 1 and Read 2 (merge_next_seq_gzip_files.py in the PHYLUCE package: https://github.com/faircloth-lab/phyluce/). Sequencing produced an average of 2,116,046 million reads (95 CI: 104,351; Table S4) per sample. We trimmed FASTQ data for adapter contamination and low-quality bases using a parallel wrapper (https://github.com/faircloth-lab/illumiprocessor) around Trimmomatic (Bolger et al. 2014). Following read trimming, we computed summary statistics on the data using get_fastq_stats.py from the PHYLUCE package, and trimmed reads averaged 139 bp in length (95 CI: 0.5; Table S4). We assembled the read data into contigs (Table S5) using a parallel wrapper around Trinity [version trinityrnaseq-r2013-02-25; assemblo_trinity.py), and we computed coverage across assembled contigs using a program (get_trinity_coverage.py) that re-aligns the trimmed sequence reads to each set of assembled contigs using BWA-MEM (Li 2013), cleans the resulting BAM files using PICARD (version 1.99; http://picard.sourceforge.net/), adds read-group (RG) information to each library using PICARD, indexes the resulting BAM file using SAMTOOLS, and calculates coverage at each base of each assembled contig using GATK [version 2.7.2. Trinity assembly of reads

produced an average of 22,100 contigs (95 CI: 1,484) of 338 bp in length (95 CI: 4.7; Supp Table BCF3).

To identify assembled contigs representing enriched UCE loci from each species, we aligned species-specific contig assemblies from both sequence assembly programs to a FASTA file of all enrichment baits using match_contigs_to_loci.py. We enriched an average of 1,040 unique UCE loci (Table S6) from each sample (95 CI: 2.7) having an average length of 668 bp (95 CI: 12.9), an average coverage of 39X (95 CI: 1.7). The mean percentage of reads-on-target was 34.1 (95 CI: 1.1).

We created a file containing the names of 56 enriched taxa from which we collected data (Table S3), as well as the name of a genome-enabled cichlid that we used as an outgroup (*Oreochromis niloticus*) and from which we extracted the same UCE loci *in silico*, and we input this list to an additional program (get_match_counts.py) that queries the relational database created by matching baits to assembled contigs, as well as the relational database containing UCE match data for genome-enabled taxa, to generate a list of UCE loci shared among all taxa. We input the list of loci generated by this program to an additional program (get_fastas_from_match_counts.py) to create a monolithic FASTA file containing all UCE sequence data for all taxa. We aligned all data in the monolithic FASTA file using a parallel wrapper (seqcap_align_2.py) around MAFFT, with the built-in trimming option of the wrapper turned off and FASTA output turned on. Following alignment, we trimmed each fasta alignment using a parallel wrapper (get_gblocks_trimmed_alignments_from_untrimmed.py) around GBLOCKS (trimming parameters --b1=0.5; --b4=8) which also converted resulting alignments to NEXUS format, and we removed the locus names from all alignments (remove_locus_name_from_nexus_lines.py).

Following UCE identification, alignment, and alignment trimming steps, we created two data sets by selecting two subsets of alignments (get_only_loci_with_min_taxa.py) that were 95% (54 of 56 taxa have data present in each alignment) and 75% complete (42 of 56 taxa have data present in each alignment). We generated alignment statistics across each subset of data, and we computed the number of informative sites across all alignments in each subset using get_align_summary_data.py and get_informative_sites.py. The 95% complete data set contained 939 loci, each containing a mean of 56.4 (95 CI: 0.05) taxa. After MAFFT alignment and GBLOCKS trimming, the average locus length in the 95% data set was 549.9 bp (95 CI: 6.23) and the concatenated supermatrix was 516,305 characters in length; contained 11,508 informative sites; and contained 55,503 site patterns. The 75% complete data set contained 1,043 loci, each having a mean of 55.8 (95 CI: 0.1) taxa. After MAFFT alignment and GBLOCKS trimming, the average locus length in the 75% data set was 541.4 bp (95 CI: 6.2) and the concatenated supermatrix was 564,686 characters in length; contained 13,012 parsimony informative sites; and contained 62,897 site patterns.

Phylogenetic analyses:

We concatenated each resulting data set into a PHYLIP-formatted supermatrix (format_nexus_files_for_raxml.py). We constructed an input file for PartitionFinder [49], which we used to partition each data set using the iterative kmeans clustering algorithm [50]; RAxML; and model selection by Bayesian Information Criterion. Following partitioning, we conducted the analyses we describe for each data set (95% and 75% complete) and each partitioning scheme (partitioned and unpartitioned).

We used the RAxML 8.0.19 [29] PTHREADS binary with the GTRGAMMA site rate substitution model on single, 16 CPU, 32 GB RAM nodes (mike.hpc.lsu.edu) to conduct 20 maximum-likelihood (ML) searches for the phylogenetic tree that best fit the data. Following the best tree search, we used RAxML to generate non-parametric bootstrap replicates using the autoMRE option, which runs bootstrapping until convergence of the bootstrap replicates. Following the best tree and bootstrap replicate analyses, we reconciled the best fitting ML tree with the bootstrap replicates. We also used the MPI version of ExaBayes 1.4.1 [28] on four, 16 CPU, 32 GB RAM nodes (mike.hpc.lsu.edu) to conduct four independent runs of 1-2 M iterations each for each data set (four independent runs; burn-in: 25%; thinning = 500). We used three heated chains to sample the posterior distribution the partitioned data analyses, because, following visual inspection of traces from preliminary runs, it appeared some runs were becoming stuck in local optima. We assessed runs for convergence using visualizations of the potential scale reduction factors and the standard deviation of the split frequencies output by the *postProcParams* and *sdsf* programs from the ExaBayes package. We also visually examined traces and ESS values for estimated parameters using Tracer [51]. We created a consensus tree from the independent runs using the *consense* program from the ExaBayes package (Figure S1, Figure S2).

The RAxML bootstrap replicate runs of all four data sets converged after 300 replicates. Bayesian analyses of the unpartitioned, 95% complete data set reached convergence (ADSF 0.001%; average PSRF =1.0 ; ±95 CI PSRF = 0.0003; average ESS = 4774.9; ±95 CI ESS=938.5) after 2 million iterations, while Bayesian analysis of the partitioned 95% complete data set (ADSF 1.2%; average PSRF =1.0 ; ±95 CI PSRF = 0.001; average ESS = 4646.3; ±95 CI ESS=223.0) reached convergence after 1 million iterations. Bayesian analyses of the unpartitioned, 75% complete data set reached convergence (ADSF 0.003%; average PSRF =1.0 ; ±95 CI PSRF = 0.0003; average ESS = 3428.7; ±95 CI ESS=631.5) after 1 million iterations, and Bayesian analysis of the partitioned 75% complete data set (ADSF 0.2%; average PSRF =1.0 ; ±95 CI PSRF = 0.0001; average ESS = 4792.8; ±95 CI ESS=148.7) reached convergence after 1 million iterations.

Converting trees to chronograms:

Prior to our phylogenetic ANOVAs (below), we used the 'chronoPL' function in R to convert our trees into chronograms using penalized likelihood. We set one calibration point at the split between Bathybates minor and the rest of the East African clade, using soft bounds of 9-12 million years, the generally accepted age of the lake. [45,52-53].

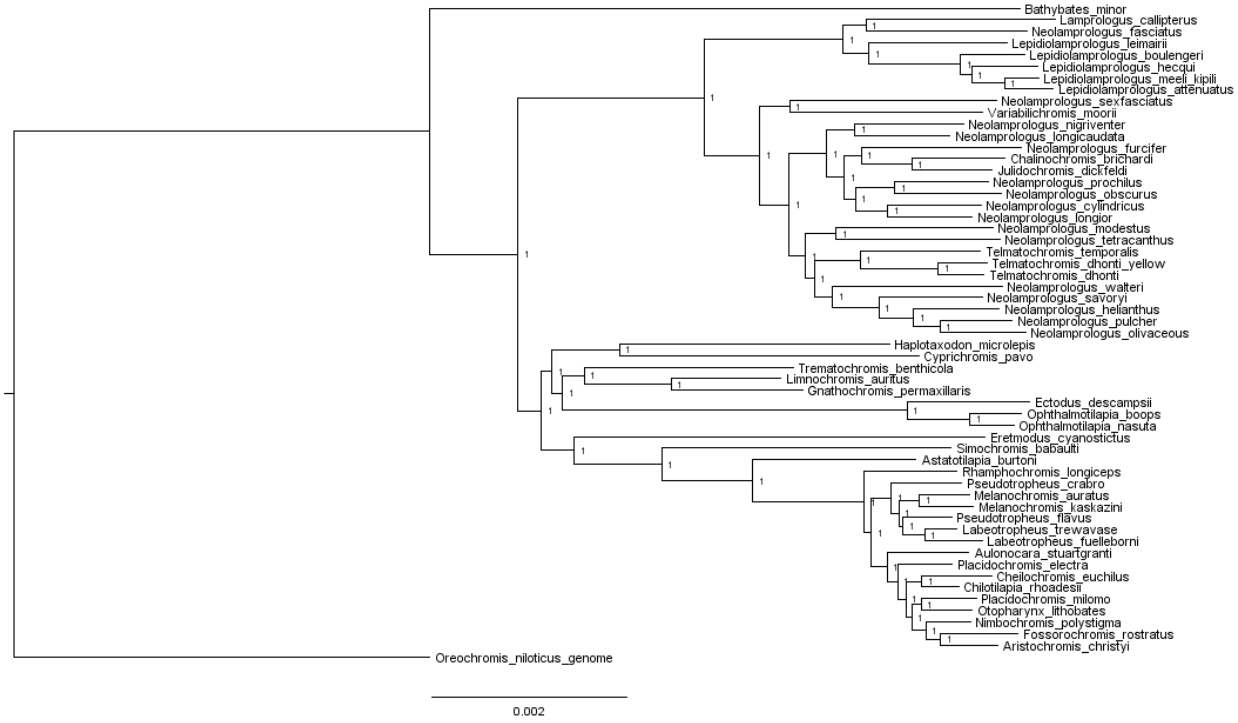

Figure S1. Consensus tree from our 95% unpartitioned ExaBayes analysis. Nodal values indicate posterior probabilities.

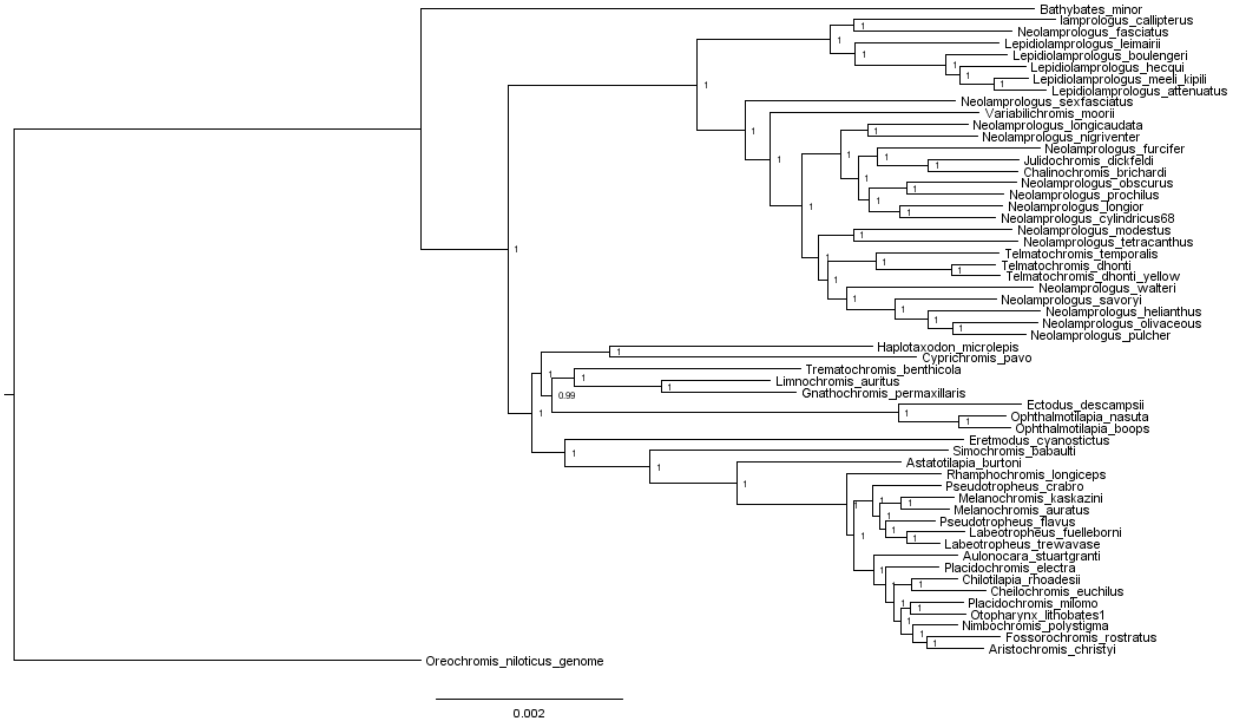

Figure S2. Consensus tree from our 75% unpartitioned ExaBayes analysis. Nodal values indicate posterior probabilities.

Identifying transitions in feeding mode:

To determine which species in our analyses were primarily biting taxa, we adopted two methodologies (Table S2). In the “strict” analysis, only herbivores and insect pickers in the rocky habitat, which feed by biting rocky surfaces, algal filaments, or freshwater sponges, were counted as biters, as this feeding mode is not known to be possible with suction feeding. We also included a molluscivorous species (*Chilotilapia rhoadesii)* known to crush snails directly with its oral jaws [16]. In the “loose” analyses, we also included two piscivorous species (*Rhamphochromis longiceps* and *Bathybates minor*) with greatly enlarged teeth on the premaxilla and dentary. These enlarged teeth suggest these two species function as “ram-biters” that overtake prey via body ram and impale prey on the oral jaw teeth. We also added two herbivorous and planktivorous species in the genus *Ophthalmotilapia* known to bite algae in the rocky habitat.

We then used stochastic character mapping in the R package ‘phytools’ [32] to map how many transitions between biting and suction feeder occurred in Tanganyika and Malawi. We split our phylogeny into Tanganyikan or Malawi species and simulated 1,000 stochastic character mappings for feeding mode based on the observed rate matrix for both the “strict” and “loose” designations with all rates allowed to differ, then recorded how many transitions occurred in each lake (Table S7). For all simulations, the minimum number of transitions was always greater than one, indicating that multiple feeding mode transitions occurred in each lake

radiation. Malawi averaged 5-6 transitions and Tanganyika averaged 7-13 across our set of RaxML/ExaBayes, 75%/95%, and unpartitioned/partitioned trees.

Comparative analysis of jaw kinesis with respect to feeding mode:

We performed phylogenetic ANOVAs on all consensus trees (75%/95%, RaxML/exaBayes, non-ultrametrized and ultrametrized) using 10,000 Brownian motion simulations with the 'aov.phylo' function in the geiger' package in R [54]. We analyzed both premaxillary kinesis and maxillary kinesis with respect to feeding mode, and used both the "strict" and "loose" designations for feeding mode. Regardless of the phylogenetic reconstruction used, (Table S8), biting taxa exhibited less premaxillary and maxillary jaw kinesis than suction feeding taxa.

Table S1. Species in the study

Species name	**Number of individuals filmed**
Aristochromis christyi	2
Astatotilapia burtoni	1
Aulonocara stuartgranti	1
Bathybates minor	1
Chalinochromis brichardi	1
Cheilochromis euchilus	1
Chilotilapia rhoadesii	1
Cyprichromis pavo	1
Ectodus descampsii	1
Eretmodus cyanostictus	1
Fossorochromis rostratus	1
Gnathochromis permaxillaris	1
Haplotaxodon microlepis	1
Julidochromis dickfeldi	1
Labeotropheus fuelleborni	1
Labeotropheus trewavasae	2
Lamprologus callipterus	3
Lamprologus fasciatus	2
Lepidiolamprologus attenuatus	2
Lepidiolamprologus boulengeri	2
Lepidiolamprologus hecqui	1
Lepidiolamprologus lemairii	2
Lepidiolamprologus sp. "meeli kipili"	3
Limnochromis auritus	2
Melanochromis auratus	1
Melanochromis kaskazini	1
Neolamprologus cylindricus	1
Neolamprologus furcifer	2
Neolamprologus helianthus	2
Neolamprologus longicaudata	4
Neolamprologus leleupi	5
Neolamprologus modestus	1
Neolamprologus nigriventris	1
Neolamprologus obscurus	3
Neolamprologus olivaceous	1
Neolamprologus prochilus	5
Neolamprologus pulcher	2
Neolamprologus savoryi	3
Neolamprologus sexfasciatus	2
Neolamprologus tetracanthus	2
Neolamprologus walteri	1
Nimbochromis polystigma	1

Ophthalmotilapia boops	1
Ophthalmotilapia nasuta	3
Otopharynx lithobates	1
Placidochromis electra	1
Placidochromis milomo	2
Pseudotropheus crabro	1
Pseudotropheus flavus	1
Rhamphochromis longiceps	1
Simochromis babaulti	1
Telmatochromis dhonti	2
Telmatochromis sp. "dhonti yellow"	2
Telmatochromis temporalis	1
Trematochromis benthicola	2
Variabilichromis moorii	3

Table S2. Biting species in two categories

Strict:	**Specialization**
Chalinochromis brichardi	Sponge-eater, algae-eater, insect picker [55]
Chilotilapia rhoadesii	Snail-eater, oral crusher [16,34]
Eretmodus cyanostictus	Algae-eater [55-57]
Julidochromis dickfeldi	Sponge-eater and insect picker[55]
Labeotropheus fuelleborni	Algae-eater [58]
Labeotropheus trewavasae	Algae-eater [34]
Melanochromis auratus	Algae-eater [58]
Pseudotropheus crabro	Parasite-eater [59]
Pseudotropheus flavus	Algae-eater [60]
Simochromis babaulti	Algae-eater [55]
Telmatochromis temporalis	Algae-eater [55-57]
Variabilichromis moorii	Algae-eater [55,57]
Loose:	
Bathybates minor	Ram-biting fish-eater [55], this study
Rhamphochromis longiceps	Ram-biting fish-eater [55], this study
Ophthalmotilapia boops	Algae-eater,plankton-eater [55]
Ophthalmotilapia nasuta	Algae-eater,plankton-eater [55-56]

Table S3. Species, location of sample collections/date of collection, identification number, processing identification number during UCE enrichment, DNA extracted, library concentration prior to PCR amplification, library concentration following PCR amplification.

Species	Location/Date Obtained	ID Number	Processing ID	DNA (ng/ul)	Pre-PCR (ng/ul)	Post-PCR (ng/ul)
Aristochromis christyi	Chinyamwezi, 25 May 2010	4828	ID25	53.3	20.3	43.7
Astatotilapia burtoni	Aquarium strain, Ruziba River	4358	ID32	46.1	20.8	58.4
Aulonocara stuartgranti	Chinyamwezi, 25 May 2010	4837	ID26	93	20.8	55
Bathybates minor	Lake Tanganyika	MDM16	ID90	219	18.7	52.4
Chalinochromis brichardi	Lake Tanganyika	4445	ID57	5.59	7.02	45.1
Cheilochromis euchilus	Chinyamwezi, 25 May 2010	4812	ID23	92.9	20.4	42.4
Chilotilapia rhoadesii	Chinyamwezi, 25 May 2010	4829	ID24	42.9	21.1	43.1
Cyprichromis pavo	Lake Tanganyika	MDM10	ID84	55.4	26	49.6
Ectodus descampsii	Lake Tanganyika	4443	ID55	15.8	15.5	43.8
Eretmodus cyanostictus	Lake Tanganyika	MDM08	ID82	84.2	21.7	49.6
Fossorochromis rostratus	Chinyamwezi, 25 May 2010	4909	ID28	84.2	26.2	56.2
Gnathochromis permaxillaris	Lake Tanganyika	4456	ID60	32.2	15.8	45.4
Haplotaxodon microlepis	Lake Tanganyika	MDM03	ID77	266	24.2	53.1
Julidochromis dickfeldi	Lake Tanganyika	4408	ID45	25.4	14.3	48.6
Labeotropheus trewavasae	Thumbi West, 18 May 2010	4377	ID6	332	21.7	49.7
Labeotropheus fullbornei	Thumbi West, 19 May 2010	4437	ID8	347	23.8	48.1
Lamprologus callipterus	Lake Tanganyika	4444	ID56	35.1	15.1	38.1
Lepidiolamprologus boulengeri	Lake Tanganyika	4396	ID36	34	25	49
Lepidiolamprologus meeli kipili	Lake Tanganyika	4403	ID40	36.2	28.1	55.8
Lepidiolamprologus attenuatus	Lake Tanganyika	4411	ID47	24.8	12.5	50.5
Lepidiolamprologus hecqui	Lake Tanganyika	4446	ID58	28.5	23.8	47.7
Lepidiolamprologus	Lake Tanganyika	4503	ID69	84.5	27.4	54.4

leimairii						
Limnochromis auritus	Lake Tanganyika	4401	ID38	19	25	54.5
Melanochromis kaskazini	Lake Malawi	4361	ID33	32.6	20.9	48
Melanochromis auratus	Thumbi West, 18 May 2010	4358	ID4	126	20.4	49.5
Neolamprologus longior	Lake Tanganyika	4367	ID35	35.7	24.7	52.4
Neolamprologus savoryi	Lake Tanganyika	4402	ID39	22.9	14.6	50.7
Neolamprologus pulcher	Lake Tanganyika	4405	ID42	21.5	6.56	52.5
Neolamprologus tetracanthus	Lake Tanganyika	4410	ID46	21.1	11.7	59.5
Neolamprologus prochilus	Lake Tanganyika	4435	ID51	50.5	23.6	50.6
Neolamprologus walteri	Lake Tanganyika	4440	ID52	41.4	20.8	48.7
Neolamprologus obscurus	Lake Tanganyika	4441	ID53	24	14.7	54.4
Neolamprologus longicaudata	Lake Tanganyika	4442	ID54	17.7	15.6	42.6
Neolamprologus modestus	Lake Tanganyika	4466	ID61	38.8	24.4	51.3
Neolamprologus sexfasciatus	Lake Tanganyika	4481	ID63	23.7	14.4	48.3
Neolamprologus furcifer	Lake Tanganyika	4498	ID66	32.6	22.5	46.6
Neolamprologus nigriventer	Lake Tanganyika	4499	ID67	74.2	25.1	56.2
Neolamprologus cylindricus	Lake Tanganyika	4502	ID68	33.9	25.7	51.5
Neolamprologus helianthus	Lake Tanganyika	MDM09	ID83	90.1	23.5	51.1
Neolamprologus olivaceous	Lake Tanganyika	MDM11	ID85	46.2	24.8	53.1
Neolamprologus fasciatus	Lake Tanganyika	MDM12	ID86	59	19.5	47
Nimbochromis polystigma	Otter Point, 18 May 2010	4336	ID2	145	21.3	46.6
Ophthalmotilapia nasuta	Lake Tanganyika	4400	ID37	95	27.4	59.2
Ophthalmotilapia boops	Lake Tanganyika	4407	ID44	11.7	3.23	51.2
Otopharynx lithobates	Mumbo Island, 24 May 2010	4605	ID16	170	19.2	48.9

Placidochromis milomo	Chinyamwezi, 25 May 2010	4630	ID17	86.6	27.7	54.3
Placidochromis electra	Chinyamwezi, 25 May 2010	4720	ID21	106	22	44.7
Pseudotropheus flavus	Chinyamwezi, 25 May 2010	4662	ID19	167	20.8	44.5
Pseudotropheus crabro	Chinyamwezi, 25 May 2010	4850	ID27	160	24.5	51
Rhamphochromis longiceps	Lake Malawi	MDM07	ID81	570	23.2	48.8
Simochromis babaulti	Lake Tanganyika	4413	ID48	37.4	21.2	49.3
Telmatochromis dhonti	Lake Tanganyika	4406	ID43	36.3	14.8	49.7
Neolamprologus niger	Lake Tanganyika	4454	ID59	21.2	13.7	46
Telmatochromis temporalis	Lake Tanganyika	4483	ID64	23.7	14.8	50.4
Trematochromis benthicola	Lake Tanganyika	MDM04	ID78	600	15	42.9
Variabilichromis moorii	Lake Tanganyika	4237	ID31	26.3	8.77	48.4

Table S4. Species, processing identification, number of sequence reads, total base pairs sequences, mean read length, 95% confidence interval of mean read length, mininimum read length, maximum read length, and median read length for sequence reads generated from cichlid UCE enrichments.

Species	Processing ID	Reads	Total BP	Avg Read Len	95 CI Read Len	Min	Max	Median
Aristochromis christyi	ID25	2,778,503	384,269,509	138.30	0.01	40	151	151
Astatotilapia burtoni	ID32	2,186,967	298,744,995	136.60	0.02	40	151	151
Aulonocara stuartgranti	ID26	2,090,484	288,888,592	138.19	0.02	40	151	151
Bathybates minor	ID90	2,213,477	303,924,012	137.31	0.02	40	151	151
Chalinochromis brichardi	ID57	2,660,775	371,056,853	139.45	0.01	40	151	151
Cheilochromis euchilus	ID23	2,364,070	326,628,349	138.16	0.02	40	151	151
Chilotilapia rhoadesii	ID24	2,609,155	362,113,768	138.79	0.01	40	151	151
Cyprichromis pavo	ID84	1,948,095	267,619,241	137.37	0.02	40	151	151
Ectodus descampsii	ID55	2,337,313	318,173,470	136.13	0.02	40	151	151
Eretmodus cyanostictus	ID82	2,426,788	339,248,936	139.79	0.01	40	151	151
Fossorochromis rostratus	ID28	1,604,350	224,069,844	139.66	0.02	40	151	151
Gnathochromis permaxillaris	ID60	2,671,626	360,266,846	134.85	0.02	40	151	151

Haplotaxodon microlepis	ID77	2,121,012	297,046,851	140.05	0.02	40	151	151
Julidochromis dickfeldi	ID45	2,797,783	388,236,278	138.77	0.01	40	151	151
Labeotropheus fullbornei	ID8	2,584,037	359,831,288	139.25	0.01	40	151	151
Labeotropheus trewavasae	ID6	2,290,040	315,556,081	137.80	0.02	40	151	151
Lamprologus callipterus	ID56	2,609,046	355,851,467	136.39	0.02	40	151	151
Lepidiolamprologus attenuatus	ID47	2,567,548	369,729,360	144.00	0.01	40	151	151
Lepidiolamprologus boulengeri	ID36	2,325,594	334,638,334	143.89	0.01	40	151	151
Lepidiolamprologus hecqui	ID58	1,476,483	208,896,042	141.48	0.02	40	151	151
Lepidiolamprologus leimairii	ID69	1,821,110	260,790,073	143.20	0.02	40	151	151
Lepidiolamprologus meeli kipili	ID40	1,040,923	148,527,034	142.69	0.02	40	151	151
Limnochromis auritus	ID38	2,298,173	319,133,446	138.86	0.02	40	151	151
Melanochromis auratus	ID4	2,492,073	345,664,041	138.71	0.02	40	151	151
Melanochromis kaskazini	ID33	2,378,319	323,751,858	136.13	0.02	40	151	151
Neolamprologus cylindricus	ID68	1,497,777	204,860,471	136.78	0.02	40	151	151
Neolamprologus fasciatus	ID86	2,095,568	289,929,496	138.35	0.02	40	151	151
Neolamprologus furcifer	ID66	1,649,214	229,038,482	138.88	0.02	40	151	151
Neolamprologus helianthus	ID83	2,494,638	348,418,953	139.67	0.01	40	151	151
Neolamprologus longicaudata	ID54	1,628,160	226,935,036	139.38	0.02	40	151	151
Neolamprologus longior	ID35	1,678,308	231,706,435	138.06	0.02	40	151	151
Neolamprologus modestus	ID61	1,491,548	204,247,477	136.94	0.02	40	151	151
Neolamprologus nigriventer	ID67	1,597,097	221,546,085	138.72	0.02	40	151	151
Neolamprologus obscurus	ID53	1,318,123	184,320,134	139.84	0.02	40	151	151
Neolamprologus olivaceous	ID85	1,745,612	240,434,330	137.74	0.02	40	151	151
Neolamprologus prochilus	ID51	2,156,968	298,551,871	138.41	0.02	40	151	151
Neolamprologus pulcher	ID42	1,902,715	259,734,882	136.51	0.02	40	151	151

Neolamprologus savoryi	ID39	2,140,419	300,298,762	140.30	0.02	40	151	151
Neolamprologus sexfasciatus	ID63	1,801,236	249,218,676	138.36	0.02	40	151	151
Neolamprologus tetracanthus	ID46	1,874,707	261,972,747	139.74	0.02	40	151	151
Neolamprologus walteri	ID52	1,843,974	256,532,675	139.12	0.02	40	151	151
Nimbochromis polystigma	ID2	2,379,346	331,765,245	139.44	0.02	40	151	151
Ophthalmotilapia boops	ID44	2,710,042	374,104,644	138.04	0.01	40	151	151
Ophthalmotilapia nasuta	ID37	2,260,275	315,306,302	139.50	0.02	40	151	151
Otopharynx lithobates	ID16	2,009,376	277,425,669	138.07	0.02	40	151	151
Placidochromis electra	ID21	2,292,954	316,558,784	138.06	0.02	40	151	151
Placidochromis milomo	ID17	1,878,364	262,502,473	139.75	0.02	40	151	151
Psedotropheus crabro	ID27	1,884,663	262,553,523	139.31	0.02	40	151	151
Pseudotropheus flavus	ID19	2,267,764	312,491,965	137.80	0.02	40	151	151
Rhamphochromis longiceps	ID81	2,304,398	320,354,921	139.02	0.02	40	151	151
Simochromis babaulti	ID48	2,023,267	274,867,011	135.85	0.02	40	151	151
Telmatochromis dhonti	ID43	1,885,260	263,341,038	139.68	0.02	40	151	151
Neolamprologus "dhonti yellow"	ID59	2,279,716	318,118,281	139.54	0.02	40	151	
Telmatochromis temporalis	ID64	1,976,770	273,439,037	138.33	0.02	40	151	151
Trematochromis benthicola	ID78	2,201,701	305,001,070	138.53	0.02	40	151	151
Variabilichromis moorii	ID31	2,534,848	352,231,624	138.96	0.01	40	151	151

Table S5. Species, processing identifications, number of contigs assembled from raw fastq reads, total number of base pairs in all contigs, average contig length, 95% confidence interval of the contig length, minimum contig length, maximum contig length, median contig length, and number of contigs >1Kb in length following assembly of raw reads sequenced from cichlid libraries enriched for UCEs.

Species	Processing ID	Contigs	Total BP	Avg Len	95 CI Avg Len	Min	Max	Median	Contigs > 1 Kb
Aristochromis christyi	ID25	31,525	10,440,130	331.2	1.9	201	16,605	244	771
Astatotilapia burtoni	ID32	21,449	6,940,281	323.6	2.1	201	16,583	241	481

Aulonocara stuartgranti	ID26	20,391	7,333,426	359.6	3.0	201	16,606	247	646
Bathybates minor	ID90	20,919	7,069,007	337.9	2.3	201	8,586	242	583
Chalinochromis brichardi	ID57	31,624	9,505,725	300.6	1.4	201	16,574	239	420
Cheilochromis euchilus	ID23	23,422	8,556,432	365.3	2.9	201	16,583	247	821
Chilotilapia rhoadesii	ID24	26,778	9,763,552	364.6	2.8	201	16,598	246	945
Cyprichromis pavo	ID84	19,193	6,587,878	343.2	2.6	201	11,087	244	514
Ectodus descampsii	ID55	23,907	7,727,800	323.2	2.1	201	16,623	240	487
Eretmodus cyanostictus	ID82	26,658	9,113,072	341.9	2.4	201	16,602	242	780
Fossorochromis rostratus	ID28	14,383	5,291,664	367.9	3.1	201	16,605	250	485
Gnathochromis permaxillaris	ID60	28,882	10,146,677	351.3	2.5	201	16,600	243	926
Haplotaxodon microlepis	ID77	22,581	7,524,953	333.2	2.4	201	8,217	243	513
Julidochromis dickfeldi	ID45	32,620	10,028,460	307.4	1.5	201	16,604	241	499
Labeotropheus fullbornei	ID8	27,810	9,470,914	340.6	2.1	201	16,602	246	777
Labeotropheus trewavase	ID6	22,484	8,513,140	378.6	3.0	201	16,602	251	919
Lamprologus callipterus	ID56	29,897	8,962,195	299.8	1.6	201	16,605	239	395
Lepidiolamprologus "meeli kipili"	ID40	12,001	3,990,816	332.5	2.6	201	8,467	245	227
Lepidiolamprologus attenuatus	ID47	36,273	11,759,787	324.2	1.7	201	16,606	246	816
Lepidiolamprologus boulengeri	ID36	30,287	9,646,327	318.5	1.6	201	16,595	246	558
Lepidiolamprologus hecqui	ID58	19,279	6,155,500	319.3	2.2	201	11,649	243	341
Lepidiolamprologus leimairii	ID69	23,762	7,678,253	323.1	1.8	201	8,037	245	488
Limnochromis auritus	ID38	25,573	9,014,605	352.5	3.0	201	16,622	244	796
Melanochromis	ID4	26,060	9,269,240	355.7	2.5	201	16,601	248	876

auratus									
Melanochromis kaskazini	ID33	24,037	8,317,847	346.0	2.3	201	16,602	246	726
Neolamprologus cylindricus	ID68	13,059	4,528,312	346.8	2.9	201	8,414	245	353
Neolamprologus fasciatus	ID86	21,444	6,651,970	310.2	1.8	201	16,607	240	338
Neolamprologus furcifer	ID66	14,724	4,977,770	338.1	2.5	201	16,598	245	342
Neolamprologus helianthus	ID83	30,224	9,451,002	312.7	1.6	201	16,594	242	496
Neolamprologus longicaudata	ID54	16,155	5,309,657	328.7	2.5	201	16,584	242	321
Neolamprologus longior	ID35	15,237	5,223,253	342.8	2.7	201	16,558	247	387
Neolamprologus modestus	ID61	13,389	4,377,047	326.9	2.7	201	16,582	243	207
Neolamprologus nigriventer	ID67	14,565	5,036,762	345.8	2.9	201	16,606	245	393
Neolamprologus obscurus	ID53	10,717	3,826,354	357.0	3.5	201	16,600	248	297
Neolamprologus olivaceous	ID85	16,517	5,269,291	319.0	2.1	201	12,553	241	313
Neolamprologus prochilus	ID51	22,142	7,329,252	331.0	2.1	201	16,585	244	544
Neolamprologus pulcher	ID42	18,693	5,949,224	318.3	2.4	201	16,599	240	324
Neolamprologus savoryi	ID39	21,732	7,176,665	330.2	2.1	201	8,396	244	495
Neolamprologus sexfasciatus	ID63	17,017	5,958,709	350.2	2.8	201	16,605	246	493
Neolamprologus tetracanthus	ID46	17,544	5,831,425	332.4	2.6	201	16,588	243	363
Neolamprologus walteri	ID52	17,904	5,980,409	334.0	2.5	201	16,597	244	424
Nimbochromis polystigma	ID2	24,437	8,768,918	358.8	2.4	201	16,605	248	843
Ophthalmotilapia boops	ID44	28,348	9,606,345	338.9	2.1	201	16,589	243	834
Ophthalmotilapia nasuta	ID37	23,768	8,245,587	346.9	2.5	201	16,599	245	736

Otopharynx lithobates	ID16	19,267	7,036,204	365.2	2.9	201	16,593	249	701
Placidochromis electra	ID21	23,931	8,331,946	348.2	2.4	201	16,601	248	660
Placidochromis milomo	ID17	19,033	6,599,783	346.8	2.5	201	6,250	245	557
Pseudotropheus crabro	ID27	18,619	6,768,070	363.5	2.9	201	16,217	250	619
Pseudotropheus flavus	ID19	22,655	8,033,516	354.6	2.6	201	16,602	247	727
Rhamphochromis longiceps	ID81	24,919	8,626,136	346.2	2.1	201	8,171	247	745
Simochromis babaulti	ID48	19,549	6,394,428	327.1	2.8	201	10,438	242	389
Telmatochromis dhonti	ID43	18,748	6,106,176	325.7	2.0	201	15,237	243	362
Neolamprologus "dhonti yellow"	ID59	23,607	7,939,813	336.3	2.2	201	16,565	243	
Telmatochromis temporalis	ID64	17,951	6,169,157	343.7	2.6	201	16,606	245	503
Trematochromis benthicola	ID78	23,032	7,888,815	342.5	2.3	201	8,392	245	629
Variabilichromis moorii	ID31	26,899	8,204,849	305.0	1.6	201	16,605	241	395

Table S6. Species, processing identification, number of contigs that are enriched UCEs, total BP UCE contigs, average length of UCE contigs, 95% confidence interval of UCE contig length, minimum UCE contig length, maximum UCE contig length, median UCE contig length, number of UCEs > 1 Kb in length, UCE contig coverage, the percentage of sequenced reads on target for UCE loci enriched from cichlid libraries.

Species	ID	UCE contigs	Total BP	Avg Len	Avg Len 95 CI	Min	Max	Median	Contigs > 1 Kb	UCE contigs coverage (x)	UCE contigs reads on target
Aristochromis christyi	ID25	1,043	723,158	693.3	4.3	221	1,366	701	13	43.9	28%
Astatotilapia burtoni	ID32	1,047	660,859	631.2	3.9	206	1,130	642	3	38.8	32%
Aulonocara stuartgranti	ID26	1,042	676,193	648.9	5.0	216	3,831	652	4	32.6	29%
Bathybates minor	ID90	1,045	698,878	668.8	4.3	229	1,017	683	2	38.8	32%

Chalinochromis brichardi	ID57	1,032	709,130	687.1	4.4	217	1,170	693	16	52.6	36%
Cheilochromis euchilus	ID23	1,042	718,286	689.3	4.3	246	1,231	697	8	34.3	28%
Chilotilapia rhoadesii	ID24	1,042	746,078	716.0	4.6	203	1,580	727	19	34.1	27%
Cyprichromis pavo	ID84	1,055	658,992	624.6	3.8	201	976	631	0	38.2	35%
Ectodus descampsii	ID55	1,050	660,047	628.6	3.7	251	1,006	639	1	41.7	32%
Eretmodus cyanostictus	ID82	1,039	718,909	691.9	3.9	221	1,102	697	7	40.2	32%
Fossorochromis rostratus	ID28	1,040	696,683	669.9	4.9	217	3,328	682	4	29	33%
Gnathochromis permaxillaris	ID60	1,035	682,141	659.1	4.0	251	1,053	666	2	44	30%
Haplotaxodon microlepis	ID77	1,044	721,634	691.2	4.7	206	3,068	705	4	33.9	33%
Julidochromis dickfeldi	ID45	1,030	740,606	719.0	4.3	239	1,093	727	13	44	32%
Labeotropheus fullbornei	ID8	1,036	735,948	710.4	4.3	217	1,223	720	8	42.1	31%
Labeotropheus trewavasae	ID6	1,036	727,421	702.1	4.2	257	1,168	711	10	37.4	30%
Lamprologus callipterus	ID56	1,024	673,541	657.8	3.9	225	1,224	665	2	55.7	37%
Lepidiolamprologus "meeli kipili"	ID40	1,048	636,236	607.1	3.4	239	953	613	0	36.2	48%
Lepidiolamprologus attenuatus	ID47	1,019	807,692	792.6	4.4	221	1,546	802	58	58.4	39%
Lepidiolamprologus boulengeri	ID36	1,012	808,038	798.5	4.5	237	1,515	812	56	57.4	41%
Lepidiolamprologus hecqui	ID58	1,052	652,818	620.5	3.5	252	991	626	0	43.3	42%
Lepidiolamprologus leimairii	ID69	1,043	732,820	702.6	3.8	252	1,029	710	1	48.7	41%
Limnochromis auritus	ID38	1,047	674,027	643.8	3.7	250	1,076	650	2	37.7	31%
Melanochromis auratus	ID4	1,039	716,496	689.6	4.4	210	1,098	704	7	38.6	29%
Melanochromis kaskazini	ID33	1,041	683,804	656.9	4.0	207	1,040	665	3	40.6	30%

Neolamprologus cylindricus	ID68	1,046	624,686	597.2	3.6	214	970	601	0	34.1	40%
Neolamprologus fasciatus	ID86	1,035	675,017	652.2	3.9	210	1,063	657	3	41.3	37%
Neolamprologus furcifer	ID66	1,045	684,308	654.8	4.1	225	992	660	0	32.8	37%
Neolamprologus helianthus	ID83	1,025	708,423	691.1	4.0	265	1,144	699	9	47.9	35%
Neolamprologus longicaudata	ID54	1,055	617,134	585.0	3.5	221	1,004	592	1	34.4	37%
Neolamprologus longior	ID35	1,047	693,770	662.6	4.0	205	1,023	670	2	34.4	39%
Neolamprologus modestus	ID61	1,061	613,682	578.4	3.6	202	964	585	0	32.2	39%
Neolamprologus nigriventer	ID67	1,053	655,140	622.2	3.7	218	1,211	631	1	32.6	37%
Neolamprologus obscurus	ID53	1,036	612,035	590.8	4.2	218	1,164	600	2	25	37%
Neolamprologus olivaceous	ID85	1,054	598,475	567.8	3.5	213	976	567	0	34.7	35%
Neolamprologus prochilus	ID51	1,052	675,683	642.3	3.8	203	985	651	0	33.8	31%
Neolamprologus pulcher	ID42	1,056	616,008	583.3	3.6	203	1,524	585	1	34.4	35%
Neolamprologus savoryi	ID39	1,030	720,632	699.6	4.2	267	1,036	714	8	33.1	33%
Neolamprologus sexfasciatus	ID63	1,045	671,603	642.7	4.0	212	1,051	643	1	35.4	36%
Neolamprologus tetracanthus	ID46	1,030	692,353	672.2	4.2	214	1,005	681	1	33.1	35%
Neolamprologus walteri	ID52	1,042	676,383	649.1	4.0	210	1,035	657	3	33	35%
Nimbochromis polystigma	ID2	1,042	759,243	728.6	5.9	227	3,814	740	14	42.3	33%
Ophthalmotilapia boops	ID44	1,034	728,461	704.5	4.3	202	1,136	714	9	40.7	29%
Ophthalmotilapia nasuta	ID37	1,035	690,240	666.9	4.1	209	2,331	673	2	36.9	31%
Otopharynx lithobates	ID16	1,042	702,092	673.8	4.3	203	1,768	677	6	33.5	31%
Placidochromis electra	ID21	1,037	748,170	721.5	4.3	214	1,182	735	10	41.2	33%

Placidochromis milomo	ID17	1,049	667,032	635.9	4.0	213	983	648	0	40.3	34%
Pseudotropheus crabro	ID27	1,046	715,944	684.5	4.3	202	1,217	698	7	33.5	34%
Pseudotropheus flavus	ID19	1,042	723,596	694.4	4.3	204	1,182	708	9	35.7	31%
Rhamphochromis longiceps	ID81	1,047	721,226	688.9	5.1	203	3,862	702	9	41.4	31%
Simochromis babaulti	ID48	1,047	626,301	598.2	3.4	225	1,048	603	1	42.8	31%
Neolamprologus "dhonti yellow"	ID59	1,022	705,661	690.5	4.1	278	1,182	694	7	39.9	36%
Telmatochromis temporalis	ID64	1,019	693,763	680.8	4.1	227	1,062	686	3	37.7	35%
Trematochromis benthicola	ID78	1,036	730,428	705.0	4.5	202	2,051	720	10	43.2	36%
Variabilichromis moorii	ID31	1,019	789,959	775.2	4.9	236	1,290	789	49	43.2	37%
Oreochromis niloticus (genome)		1,014	2,195,651	2,165.3	1.1	1522	2,242	2,177	1,014		

Table S7. Character state transitions observed in sets of 1000 stochastic character mapping simulations on the following ultrametric trees.

	Min	*Mean*	*Med.*	*Max*
Malawi:				
Biting categorization, strict:				
75% unpartitioned, RaxML	3	5.414	5	15
95% unpartitioned, RaxML	3	5.445	5	15
75% partitioned, RaxML	3	5.644	5	16
95% partitioned, RaxML	3	5.785	5	12
75% unpartitioned, exaBayes	3	5.796	6	14
95% unpartitioned, exaBayes	3	5.843	6	14
75% partitioned, exaBayes	3	5.775	6	13
95% partitioned, exaBayes	3	5.891	6	13
Biting categorization, loose:				
75% unpartitioned, RaxML	3	4.927	5	12
95% unpartitioned, RaxML	3	5.018	5	12

75% partitioned, RaxML	3	4.978	5	14
95% partitioned, RaxML	3	5.680	5	14
75% unpartitioned, exaBayes	3	5.854	6	16
95% unpartitioned, exaBayes	3	5.958	6	17
75% partitioned, exaBayes	3	5.812	6	17
95% partitioned, exaBayes	3	6.116	6	15
*Tanganyika**:***				
Biting categorization, strict:				:
75% unpartitioned, RaxML	5	13.569	13	30
95% unpartitioned, RaxML	5	13.238	13	31
75% partitioned, RaxML	5	12.035	12	24
95% partitioned, RaxML	5	10.885	11	24
75% unpartitioned, exaBayes	5	12.507	12	28
95% unpartitioned, exaBayes	5	10.957	11	26
75% partitioned, exaBayes	5	13.143	13	27
95% partitioned, exaBayes	5	10.802	10	25
Biting categorization, loose:				
75% unpartitioned, RaxML	6	7.220	7	14
95% unpartitioned, RaxML	6	7.208	6	14
75% partitioned, RaxML	6	8.428	8	19
95% partitioned, RaxML	6	8.267	8	17
75% unpartitioned, exaBayes	6	8.163	8	14
95% unpartitioned, exaBayes	6	8.074	8	17
75% partitioned, exaBayes	6	8.167	8	19
95% partitioned, exaBayes	6	7.973	8	17

Table S8. Insensitivity of phylogenetic ANOVA results regardless of the phlyogenetic reconstruction chosen. * p < 0.05, ** p < 0.01, *** p < 0.001

	effect size	**p-value**
Jaw kinesis, premaxilla		
Biting categorization, strict:		
Non-ultrametric		
75% unpartitioned, RaxML	-0.074	0.0148 *
95% unpartitioned, RaxML	-0.074	0.0149 *
75% partitioned, RaxML	-0.074	0.0155 *
95% partitioned, RaxML	-0.074	0.0113 *
75% unpartitioned, exaBayes	-0.074	0.0134 *
95% unpartitioned, exaBayes	-0.074	0.0131 *
75% partitioned, exaBayes	-0.074	0.0159 *
95% partitioned, exaBayes	-0.074	0.014 *
Ultrametric		
75% unpartitioned, RaxML	-0.074	0.0133 *
95% unpartitioned, RaxML	-0.074	0.0131 *
75% partitioned, RaxML	-0.074	0.0153 *

95% partitioned, RaxML	-0.074	0.0143 *
75% unpartitioned, exaBayes	-0.074	0.0133 *
95% unpartitioned, exaBayes	-0.074	0.0138 *
75% partitioned, exaBayes	-0.074	0.0141 *
95% partitioned, exaBayes	-0.074	0.0153 *
Biting categorization, loose:		
Non-ultrametric		
75% unpartitioned, RaxML	-0.089	0.0016 **
95% unpartitioned, RaxML	-0.089	0.001 **
75% partitioned, RaxML	-0.089	0.0018 **
95% partitioned, RaxML	-0.089	0.0015 **
75% unpartitioned, exaBayes	-0.089	0.0015 **
95% unpartitioned, exaBayes	-0.089	0.0015 **
75% partitioned, exaBayes	-0.089	0.0014 **
95% partitioned, exaBayes	-0.089	0.002 **
Ultrametric		
75% unpartitioned, RaxML	-0.089	0.0014 **
95% unpartitioned, RaxML	-0.089	0.0011 **
75% partitioned, RaxML	-0.089	0.0019 **
95% partitioned, RaxML	-0.089	0.0015 **
75% unpartitioned, exaBayes	-0.089	0.0021 **
95% unpartitioned, exaBayes	-0.089	0.0018 **
75% partitioned, exaBayes	-0.089	0.0023 **
95% partitioned, exaBayes	-0.089	0.0028 **
Jaw kinesis, maxilla		
Biting categorization, strict:		
Non-ultrametric		
75% unpartitioned, RaxML	-0.107	0.0055 **
95% unpartitioned, RaxML	-0.107	0.0052 **
75% partitioned, RaxML	-0.107	0.0063 **
95% partitioned, RaxML	-0.107	0.0056 **
75% unpartitioned, exaBayes	-0.107	0.0049 **
95% unpartitioned, exaBayes	-0.107	0.0036 **
75% partitioned, exaBayes	-0.107	0.0043 **
95% partitioned, exaBayes	-0.107	0.0049 **
Ultrametric		
75% unpartitioned, RaxML	-0.107	0.0048 **
95% unpartitioned, RaxML	-0.107	0.0048 **
75% partitioned, RaxML	-0.107	0.0047 **
95% partitioned, RaxML	-0.107	0.0048 **
75% unpartitioned, exaBayes	-0.107	0.0044 **
95% unpartitioned, exaBayes	-0.107	0.005 **
75% partitioned, exaBayes	-0.107	0.0056 **
95% partitioned, exaBayes	-0.107	0.0056 **

Biting categorization, loose:

Non-ultrametric

75% unpartitioned, RaxML	-0.099	0.014 *
95% unpartitioned, RaxML	-0.099	0.0119 *
75% partitioned, RaxML	-0.099	0.0141 *
95% partitioned, RaxML	-0.099	0.0131 *
75% unpartitioned, exaBayes	-0.099	0.0135 *
95% unpartitioned, exaBayes	-0.099	0.0155 *
75% partitioned, exaBayes	-0.099	0.0152 *
95% partitioned, exaBayes	-0.099	0.015 *

Ultrametric

75% unpartitioned, RaxML	-0.099	0.0146 *
95% unpartitioned, RaxML	-0.099	0.0131 *
75% partitioned, RaxML	-0.099	0.0124 *
95% partitioned, RaxML	0.099	.0138 *
75% unpartitioned, exaBayes	-0.099	0.0129 *
95% unpartitioned, exaBayes	-0.099	0.0151 *
75% partitioned, exaBayes	-0.099	0.0158 *
95% partitioned, exaBayes	-0.099	0.0162 *